Desalination and Water Treatment
www.deswater.com
doi: 10.5004/dwt.2020.26130

200 (2020) 205–216
October

Removal of lead ion from aqueous solutions by adsorption onto phosphate-functionalized treated waste papers (PF-TWPs)

Amir Hossein Mahvi[a,b], Mohammad Sarmadi[c,d], Daryoush Sanaei[e,*], Hamid Abdolmaleki[f]

[a]*School of Public Health, Tehran University of Medical Sciences, Tehran, Iran, email: ahmahvi@yahoo.com (A.H. Mahvi)*
[b]*Center for Solid Waste Research, Institute for Environmental Research, Tehran University of Medical Sciences, Tehran, Iran*
[c]*Department of Environmental Health Engineering, School of Health, Torbat Heydariyeh University of Medical Sciences, Torbat Heydariyeh, Iran, email: msarmadi2@gmail.com (M. Sarmadi)*
[d]*Health Sciences Research Center, Torbat Heydariyeh University of Medical Sciences, Torbat Heydariyeh, Iran*
[e]*Department of Environmental Health Engineering, School of Public Health and Safety, Shahid Beheshti University of Medical Sciences, Tehran, Iran, Tel. +98-02166954234; email: daryss2572@gmail.com (D. Sanaei)*
[f]*Department of Environmental Health Engineering, School of Public Health, Hamedan University of Medical Science, Hamedan, Iran, email: hamidabdolmaleki1368@gmail.com (H. Abdolmaleki)*

Received 8 May 2019; Accepted 14 May 2020

ABSTRACT

Waste papers, although known as a potential global concern, could be used as an adsorbent for removal of lead ions from the aqueous medium, following some degrees of modifications. The present study deals with the adsorption of Pb(II) ion from aqueous solution by using phosphate-functionalized treated waste papers (PF-TWPs). Batch adsorption study was performed based on contact time, pH, adsorbent dose, and temperature. There was logical coordination of experimental data with Freundlich and Langmuir isotherms. The results of this study showed that the percentage of Pb(II) adsorption on the PF-TWPs increased with increasing pH of approximately 5.5, higher or lower pHs showed no remarkable variation in adsorption capacity. The kinetics analysis showed a substantial correlation between the experimental adsorption data with the pseudo-second-order model. Besides, thermodynamic studies were conducted to explore the adsorption of Pb(II) onto PF-TWPs, regarding the influence of temperature on this process. The spontaneity and endothermicity of the Pb(II) adsorption process were identified based on the negative free energy value and positive enthalpy change. The result of the present study showed that the PF-TWPs could be used as a cost-effective adsorbent for Pb(II) removal from industrial effluent.

Keywords: Low-cost adsorbent; Lead(II); Waste papers; Adsorption isotherms and kinetics

1. Introduction

Over the past several decades, industrialization has been rapidly growing worldwide. The development of industrialization among modern societies has contributed to the release of numerous toxic discharges into the environment. Moreover, the lack of proper control of these pollutants leads not only to serious environmental problems but, also to life-threatening consequences in humans [1]. Currently, more than several hundred unique organic and inorganic chemical compounds have been recognized in aqueous streams [2]. Besides, heavy metals are one of the most important aqueous contaminants [3,4]. Heavy metals, as environmental contaminants, have been currently known as a major global concern [5–7]. Which can directly affect the anthropomorphic health through the consumption of

* Corresponding author.

contaminated food and water? With this in mind, the control of heavy metals has attracted particular attention over the last few years [8,9].

Lead is one of the most important and prevalent toxic heavy metals which is repeatedly used in a wide variety of industries such as tanning and leather industries, manufacturing industries, catalyst and pigments, fungicides, ceramics, crafts, glass, photography, electroplating industry and corrosion control applications [10]. Owing to the high toxicity, the capability of accumulation in the food chain, and making undesirable effects on human health such as visual disturbances, constipation, convulsions, anemia, vomiting, nausea, impaired function of brain and liver [11], abortion, still-birth, sterility and neonatal deaths [12], severe abdominal pain and gradual paralysis in the muscles, cancer, coma and renal failure, which all are as a matter of discharge of the lead-contained effluents to the environment [13]. Therefore, the elimination of lead from aqueous solutions is highly crucial [14].

The available methods aiming to remove Pb(II) from aqueous effluents are precipitation, electroplating, evaporation, coagulation, sedimentation, ion exchange, cementation, floatation, membrane separation, electrocoagulation, bio-sorption and adsorption [15–17]. However, most of these methods are expensive and, in some cases, ineffective in low concentrations [18,19]. On the other hand, adsorption processes take advantage of being cost-effective [20] and result in high-quality treated effluent [21–23]. Also, there is a great amount of lead-contained effluents that can be produced by industries or agricultural operations [24], which are readily accessible for implementation in the absorption processes [20].

Currently, a number of inexpensive materials such as apricot stone [25], bamboo charcoal [26], olive stone carbon [27], lemon peel [28], sunflower stalks [29], agricultural fibers [30], tangerine peel [31], and modified activated [32], have been applied as an adsorbent for removal of heavy metals from the aqueous solutions, attempting to find alternatives for conventional sorbent materials such as activated carbon. As regards, the discharge of heavy metals such as Pb from industrial wastewater into the aqueous system, especially in Iran is a basic environmental problem. The Environmental Protection Agency has enforced the industries to remove heavy metals from their effluents to achieve the standards of releasing the materials into the environment. The adsorption process is a simple and cost-effective method of recovering and eliminating heavy metal ions from industrial wastewater. The high price of conventional absorbent materials like activated carbon has made many industries reluctant to remove Pb(II) from their effluents.

In this study, using an adsorbent for the removal of lead was used for the first time. In this study, we have tried to highlight the role of an affordable absorbent material like waste papers for removing the Pb(II) from industrial wastewaters. Our findings can be used by the executive organization and other related companies. Papers (old newspaper, old magazine, printed papers, and mixed office waste paper) are inevitable and abundant municipally produced wastes which mainly consist of cellulose, which in turn contains functional polar groups such as alcohols and ethers. With this in mind, this study attempted to examine the reuse of waste papers as an adsorbent for the removal of lead ions, thereby assessing their efficiency for the treatment of wastewater. Phosphate-functionalized treated waste papers (PF-TWPs) is an adsorbent used for the removal of lead from aqueous solutions [33].

2. Methods and materials

2.1. Preparation of PF-TWPs

Analytical grade chemicals were used as reagents to prepare PF-TWPs adsorbent. The waste papers were collected from recycling centers in Tehran and transferred into the laboratory. Subsequently, the papers were cut into several pieces (1 cm × 1 cm) by a paper shredding machine. In order to remove foreign agents (stuck to the waste paper) such as grease, black ink, and bleaching materials were treated with a concentrated sodium bicarbonate solution. Then the mixed solution was transferred to 250 mL beakers and heated to 60°C ± 5°C and then, the ingredients of this container were mixed by a shaker for approximately 6 h to obtain a pulp.

2.2. Synthesis of PF-TWPs

The resultant waste paper pulp was refluxed with 5.0% Na_2HPO_4 for up to 4 h by using a water condenser. The aim of this action was to impregnate the phosphate into the cellulose matrix, which is called the "phosphorylation process". After this process, the solution was cooled and passed through Whatman 40 filter paper, followed by air-drying of the treated waste paper pulp and fine grinding via a mixer grinder. Meanwhile, this adsorbent was stored at an appropriate place for later use. Initially, standard stock solutions of Pb(II) (1,000 ± 2 mg L^{-1}) were prepared by dissolving weighted lead nitrate salts in distilled water. Then, the prepared aqueous solution was diluted by Milli-Q water to achieve the desired concentrations. The concentrations of metals solutions ranged from 5 to 50 mg L^{-1}.

2.3. Characterization of adsorbent

The adsorption of lead on PF-TWPs adsorbent was investigated by the batch method. The surface area of the PF-TWPs and waste paper pulp (WPs) were measured by Brunauer–Emmett–Teller (BET) nitrogen adsorption technique method using a BET, surface area analyzer (TriStar 3000, Micromeritics, surface area and pore size analyzer, U.S. Sales) in the relative pressure range of $0.05 \leq (P/P_0) \leq 0.3$. Prior to the above procedure, the adsorbent was preheated at 200°C for 4 h under vacuum condition (6.67 Pa) to clean the surface. X-ray diffractometer (Thermo Scientific ARL EQUINOX LAUE X-ray diffractometer (XRD), Netherlands) with radiation (40 kV, 30 mA) in the 2θ range of 5°–60° at a scanning rate of 3°min was used to identify the crystalline characteristic of adsorbent, and to estimate the size of crystallite. Fourier-transform infrared spectroscopy (FTIR) (Bruker Vector 22, Great Britain) was also employed to clearly demonstrate the interaction of the surface functional groups of the adsorbent with the lead ions, recording spectra in a wave-length range of 400–4,000 cm^{-1}. The surface morphology of PF-TWPs is investigated by field emission scanning electron microscopy (FE-SEM) images (FE-SEM,

JEOL 7600F, Moscow, Russia). Inductively coupled plasma optical emission spectrometer ICP–OES (SPECTRO ARCOS ICP-OES analyzer, Germany)was used to determine the concentration of lead in aqueous solutions.

2.4. Batch adsorption experiments

The adsorption experiments were performed at room temperature (25°C), with different initial concentrations of lead ions (5–50 mg L^{-1}), contact times (20–120 min), PF-TWPs doses (0.4–4 g/100 mL) and pH (2–8). The Pb(II) percent removal (%) is defined as [33]:

$$\%R(\mathrm{Pb}) = \frac{C_i - C_e}{C_i} \times 100 \quad (1)$$

The equilibrium adsorption Pb(II) capacity of the PF-TWPs per unit mass (q_e) was calculated according to the following equation:

$$q_e = \frac{C_i - C_e}{m} \times V \quad (2)$$

where C_i and C_e are the initial and final lead concentrations (mg L^{-1}), respectively, V is the total volume of solution (L), and m is the PF-TWPs dosage (g).

The study on adsorption isotherm was conducted with different initial Pb(II) concentrations (5–50 mg L^{-1}) at fixed volume (100 mL), optimal PH (5.5), PF-TWPs dose (1 g), absorption time (120 min), and at room temperature. The experiments of the kinetic adsorption model via PF-TWPs adsorbent were adjusted with the pseudo-first-order and pseudo-second-order models. These experiments were repeated three times under the same experimental condition, followed by reporting the average values. The relative standard deviation was reported to be between ±1.8% and ±2.4%.

3. Results and discussion

3.1. Characterization of PF-TWPs

The surface functional groups and structure of the material were studied by FTIR (Figs. S1and S2). The FTIR spectra of WPs and PF-TWPs were recorded between 300 and 4,000 cm^{-1} in FTIR-8400S (Shimadzu Corporation, Nakagyo-Ku, Kyoto, Japan). Nikonenko et al. [34] demonstrated that the characteristic cellulose peak located at the 1,000–1,200 cm^{-1} fingerprint region by FTIR spectra. The bands close to the 1,162 and 1,111 cm^{-1}, and those close to the 1,316 cm^{-1} could be attributed to the C–O–C groups of b-(1–4) bands and CH_2-wagging vibrations in cellulose, respectively [35]. Additionally, the bending vibration feature of absorbed water has been identified by a band at the vicinity of 1,635–1,640 cm^{-1}, with a band near 3,356 cm^{-1} demonstrating the OH vibration. Two peaks with less intensity were derived from a single WPs 3,694 cm^{-1} band, owing to the varied hydrogen bonding interactions in the intramolecular level. A band was shown to appear in the PF-TWPs: 1,027 cm^{-1} region attributing to aliphatic P–O stretching [12]. No spectral bands were found in the P–O stretching-corresponding region of 1,210 cm^{-1} from the FTIR spectra of PF-TWPs. While two depicted structures varied in the valence state, they failed to explain the reduction in P(V) to P(III). Regarding our FTIR studies, the described structure was likely to belong to the phosphorylated cellulose. However, this study failed to describe the reduction mechanism of phosphorus.

The cellulose in different papers can be distinguished by their Raman spectroscopy that is shown in Fig. 1a. As can be seen, the D and G bands of cellulose in all papers are much the same. Thermogravimetric analysis (TGA) curves of WPs and PF-TWPs are depicted in Fig. 1b. As seen, the weight losses of WPs starts at 135°C and then to be consistent with 320°C. Afterward, the weight losses dramatically declined (more than 70%). While the weight losses of PF-TWPs started at 360°C and thereafter steeply fall at 450°C. These results indicate that the modification of WPs can influence the structure of cellulose thoroughly.

To prepare the adsorbent for SEM analysis, the sample was heated at 150°C for 3 h under vacuum condition. As shown in Fig. 2, the space of fibers is filled by accumulated fine particles in the microstructures of waste papers during the modification of adsorbent with disodium phosphate.

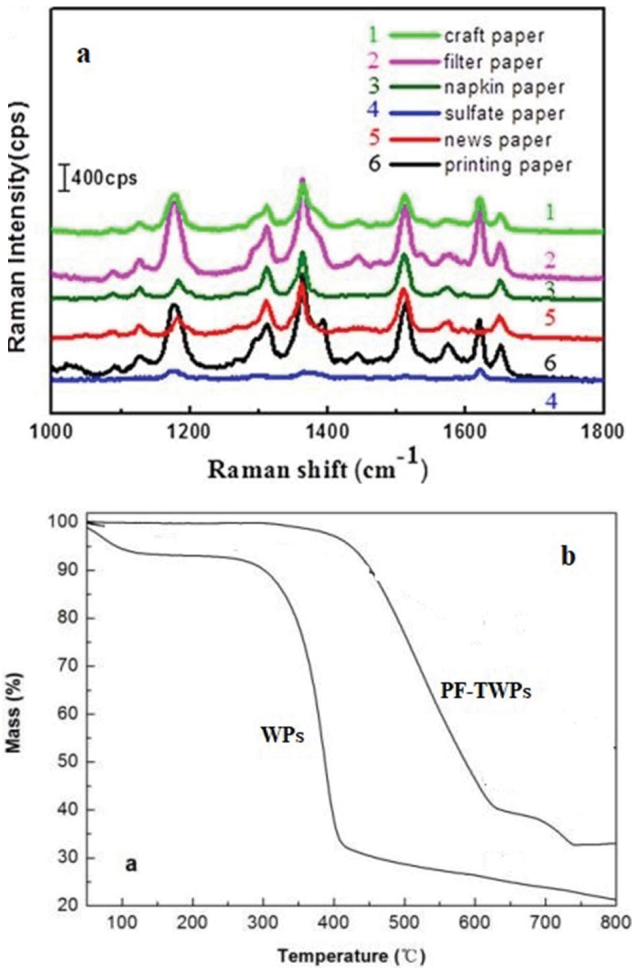

Fig. 1. (a) Surface-enhanced Raman scattering spectra on different cellulose paper and (b) TGA curves of the WPs and PF-TWPs.

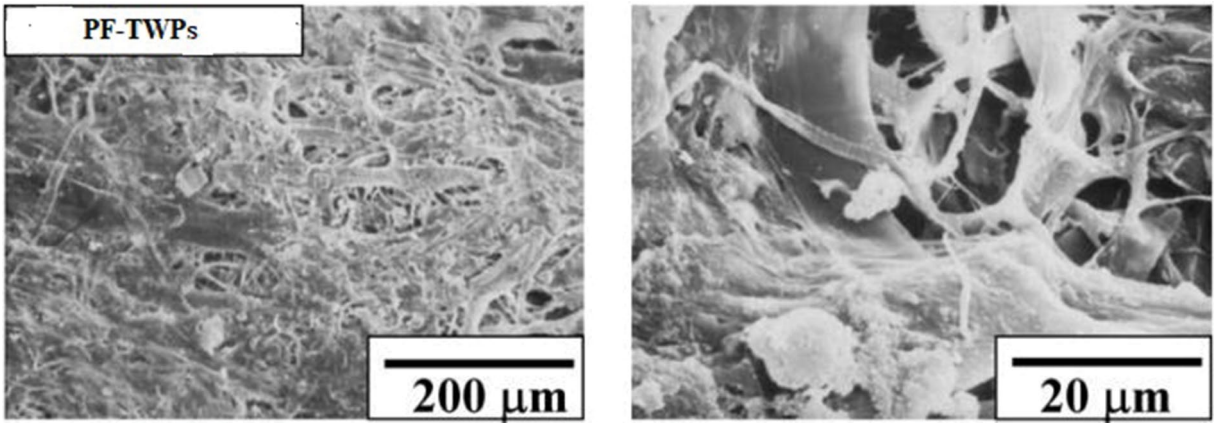

Fig. 2. FE-SEM analysis for the phosphate-functionalized treated waste papers (PF-TWPs).

The presence of cellulose matrix in WPs and PF-TWPs was checked by X-ray diffraction analysis. Through the use of this instrument, different phases for both of the above materials were demonstrated, being close to the native cellulose phases [36]. Furthermore, the presence of foreign materials in these materials resulted in the formation of three peaks (d = 3.906, 5.674, and 2.538) and several peaks with low intensity. The current study clearly indicated that pure PF-TWPs was more similar to the native form of cellulose following chemical treatment.

WPs and PF-TWPs quantitative chemical analysis (via X-ray fluorescence instrument) (Table S1 and Fig. S3) revealed that the untreated WPs including inorganic elements (iron – 0.33%, copper – 0.9%, zinc – 0.05%, magnesium – 0.56%, and manganese – 1.02%), could also be observed in PF-TWPs in a trace amount. Resemble evidence was found in WPs and PF-TWPs diffraction patterns [33]. Additionally, the presence of chemically estimated phosphorous approved its impregnation during the chemical treatment.

3.2. Effect of PF-TWPs doses and pH

The adsorbent capacity for a given initial concentration of Pb(II) ion solution was assessed based on the dosage of the adsorbent. The effects of different doses of adsorbent were explored in various concentrations of Pb(II) ions, pH 5.5, and a contact time of 120 min. The results of this study demonstrated that there was a direct association between the uptake of Pb(II) ions and the absorbent doses. The removal of Pb(II) increased from 26% to 75% at the time when the absorbent dose being increased from 0.2 to 1 g in a 1,000 mL stock solution. As depicted in Fig. 3a, the removal of Pb(II) efficiently increased with the adsorbent optimal dose (1 g L^{-1}). However, no significant change in the absorption was found in the higher concentrations of the adsorbent, which might be related to the saturation of adsorbent surface with Pb(II) ions.

Newspapers are complex materials and consist principally of cellulose which includes polar functional groups such as alcohols and ethers. These functional groups can be protonated at lower pH. In this study, the phosphate-functionalized surface of cellulose simultaneously decrease the pH and increase the functional group on the surface

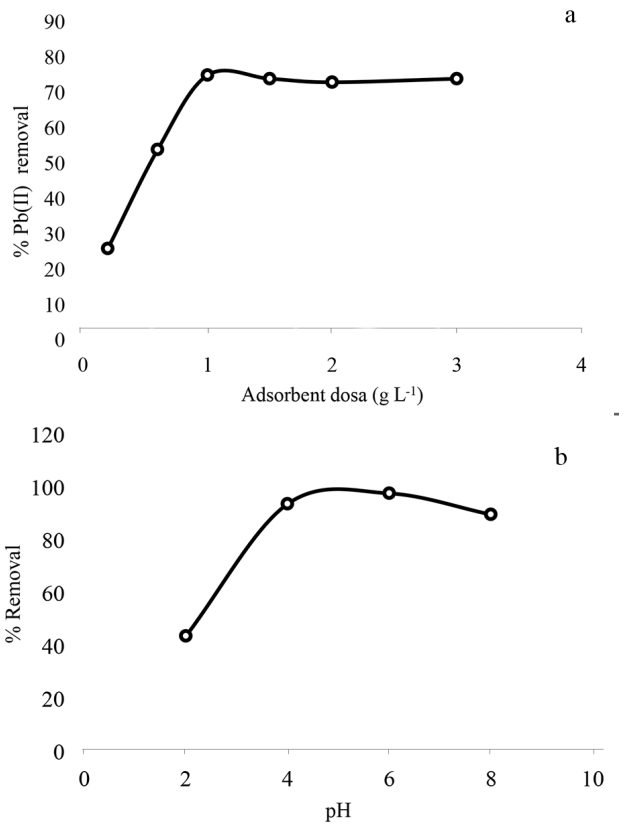

Fig. 3. Plot effects of (a) adsorbent concentrations and (b) pHs on Pb(II) adsorption by PF-TWPs.

cellulose. This functional group can be chelated with heavy metal and remove them from the solution.

A couple of studies have taken into account the pH of the aqueous solution as an important factor that controls the adsorption rate of metal ions. The effects of pH (ranged from 2 to 8) on the uptake of Pb(II) through PF-TWPs were investigated at room temperature and initial Pb(II) concentration of 5 mg L^{-1} that is shown in Fig. 3b. This experimental research showed that the maximum Pb(II) absorption (77%) on the PF-TWPs took place

at pH 5.5. At lower pH, the H_3O^+ ions compete with the Pb(II) ions to occupy the adsorption sites of PF-TWPs [6]. On the other hand, the Pb(II) adsorption efficiency onto PF-TWPs was demonstrated to be low at the high pH, which may be due to the precipitation of lead in the form of $Pb(OH)_2$ in aqueous solution [37]; thereby the adsorption efficiency of Pb(II) by PF-TWPs was reduced.

3.3. Effects of contact time

The effects of contact time (20–150 min) of Pb(II) adsorption onto PF-TWPs were explored at the initial concentration of Pb(II) (5, 20, and 50 mg L^{-1}), pH 5.5, at room temperature. Besides, the isotherm study revealed that Pb(II) adsorption onto PF-TWPs gradually increased as the contact time reached the equilibrium time (60 min) (Fig. 4). Although a higher adsorption rate was observed in a contact time of 60 min. As reported by previous studies, this high rate of Pb(II) adsorption was the result of more accessibility of active sites on the surface of PF-TWPs. At contact times longer than 60 min, the adsorption rate does not dramatically increase, which could consider equally increases in adsorption rate in equilibrium time (>60 min). The reason for this reduced adsorption rate was the decreased number of active sites.

3.4. Adsorption isotherm studies

Equilibrium isotherm models are used to identify the capacity, surface properties, and affinity of an adsorbent. Among all of the theoretical isothermal models, Langmuir, Freundlich, and Temkin isotherm models were selected to set the experimental sorption data of this study.

Meanwhile, the Langmuir equation was performed based on four basic assumptions: (1) all adsorption sites are identical and energetically equivalent; (2) there was only monomolecular layer adsorption at maximum absorption, the adsorption sites were identical; (3) there were no interactions between adsorbate molecules on adjacent sites; (4) the surface of the adsorbent was contacted with a solution containing an adsorbent enabled strongly be attracted the surface [38].

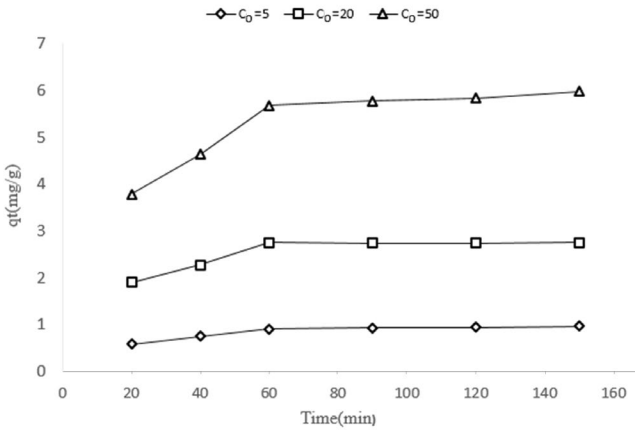

Fig. 4. Effects of contact time on adsorption Pb ions onto PF-TWPs in varied initial concentrations.

The linear Langmuir equation is written as follows:

$$\frac{C_A}{q_A} = \frac{1}{b_A Q_{\max}} + \frac{C_A}{Q_{\max}} \tag{3}$$

where q_A is equilibrium adsorbent-phase concentration of adsorbate A (mg g^{-1}), C_A is the equilibrium concentration of adsorbate A in solution (mg L^{-1}), $Q_{\max}$ is the maximum adsorbent-phase concentration of adsorbate when surface sites are saturated with adsorbate (mg g^{-1}), and b_A is Langmuir adsorption constant of adsorbate (L mg^{-1}) (Fig. 5a).

Unlike Langmuir isotherm, the Freundlich adsorption isotherm was classified as an empirical equation which takes into account various kinds of adsorption sites on the solid surface and used to describe the adsorption on the heterogeneous surface [39]. The linear form of the Freundlich isotherm equation can be written as:

$$\text{Log } q_A = \log K_A + \left(\frac{1}{n}\right)\log C_A \tag{4}$$

where K_A is a Freundlich adsorption capacity parameter (mg g^{-1}) (L mg^{-1}), and $1/n$ is a Freundlich adsorption intensity parameter (dimensionless) (Fig. 5b).

Temkin isotherm is a model that explains the effects of indirect adsorption interaction of adsorbate upon the adsorbent. Temkin [40] suggested that the heat of adsorption decreases linearly with increasing coverage and the adsorption is characterized by a uniform distribution of binding energies. The Temkin isotherm has a convenient linear form, expressed by the following equation:

$$q_e = B \ln A_T + B \ln C_e \tag{5}$$

$$B = \frac{RT}{b} \tag{6}$$

where A_T is Temkin isotherm equilibrium binding constant corresponding to the maximum binding energy (L g^{-1}), B is constantly related to the heat of sorption (J mol^{-1}), R is the universal gas constant (8.314 J mol^{-1} K^{-1}), T is the absolute temperature at 298 K, b is Temkin isotherm constant, which indicates the adsorption potential of the adsorbent. Both A_T and B can be determined from a plot q_e vs. lnC_e and the constants were determined from the intercept and slope, respectively (Fig. 5c).

The isotherm parameters for the equilibrium adsorption data of Pb(II) onto PF-TWPs are briefly presented in Table 1. The high correlation coefficient values of Freundlich and Langmuir isotherm models at all levels of temperatures showed their superiority in describing Pb(II) adsorption onto PF-TWPs, in comparison with Temkin model. The correlation coefficient, R^2 (>0.97), was also arranged to delineate the closeness of the fit data to the models. With the applicability of the Freundlich model in showing the surface heterogeneity of adsorbent, therefore, it was shown that the PF-TWPs had a heterogeneous surface. As the Freundlich constant

(1/*n*) with a 0–1 value shows the desired condition of adsorption [36]. Its calculated amount for initial concentrations of Pb(II) (5–50 mg L^{-1}) was lower than 1, exhibiting the ideal condition and usefulness PF-TWPs for the absorption of Pb(II). Moreover, the constant values *k* is another parameter of Freundlich isotherm describing the strength of the bond between the adsorbate and adsorbent. In his study, it was found that increased temperature reduces the *K* values for PF-TWPs, indicating that the adsorption process was an exothermic process. The Q_{max} and b_L Langmuir constants and their correlation coefficient for different temperatures are demonstrated in Table 1. The value of Q_{max} (mg g^{-1}) measured under the current experimental conditions was 72.46 mg g^{-1}, increasing with the increase of temperatures. This illustrates the exothermic nature of the sorption process. As shown in Table 1, an increase in temperature leads to the decreased value of constant b_L (which represents the adsorbent and adsorbate affinity).

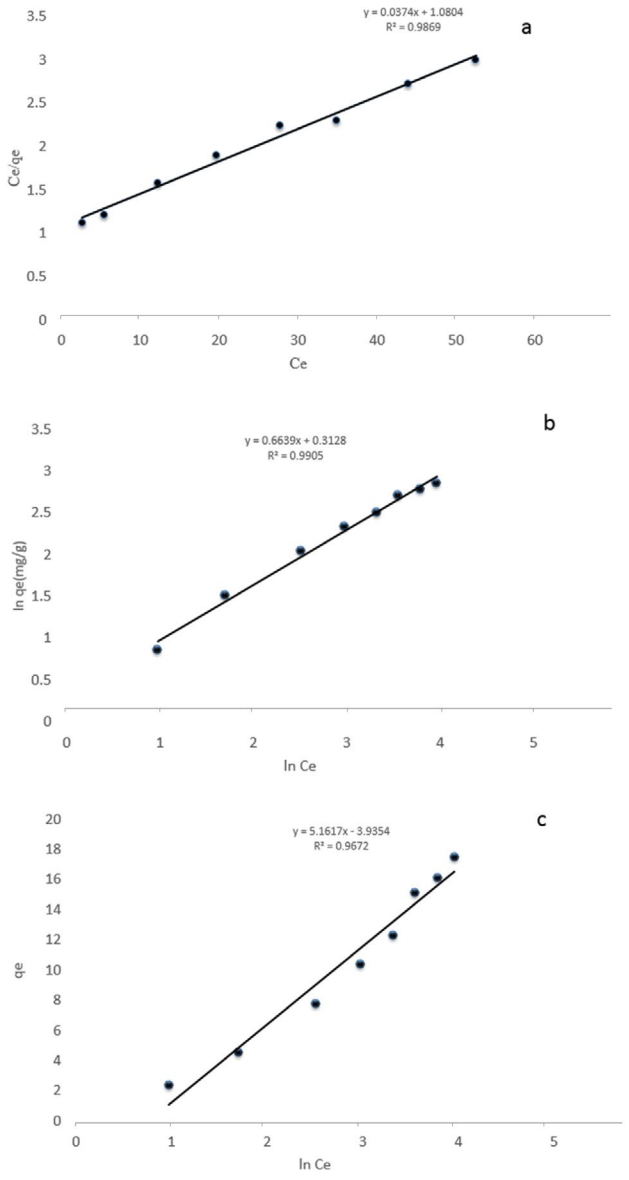

Fig. 5. (a) Langmuir, (b) Freundlich, and (c) Temkin isotherms plots of Pb removal by PF-TWPs.

3.5. Comparison with other adsorbents

Table 2 shows the comparison of the other adsorbent vs. PF-TWPs in the term of adsorption capacity of Pb(II). As shown, the higher adsorption capacity (Q_{max}) obtained in this work at room temperature and pH = 5.5 that was comparable with other adsorbents.

3.6. Adsorption kinetics and mechanism

The kinetics of Pb(II) ions adsorption onto PF-TWPs was investigated at various initial concentrations. The Lagergren pseudo-first-order [51], pseudo-second-order [52] and intraparticle diffusion [53] models were used to evaluate this process.

Lagergren pseudo-first-order model is one of the most widely used in the sorption of solid capacity-based liquid/solid systems. The linearized form of the Lagergren pseudo-first-order equation is written as follow:

$$\mathrm{Log}\left(q_e - q_t\right) = \mathrm{Log}\, q_e - \frac{k_1 t}{2.303} \tag{7}$$

where q_e (mg g^{-1}) and q_t (mg g^{-1}) are amounts of Pb(II) ions adsorbed onto PF-TWPs at equilibrium and *t* times, respectively. k_1 the Lagergren pseudo-first-order rate constant for the kinetic model (min^{-1}). The rate constant k_1 and q_e can be, respectively, calculated by the slope and intercept of the linear plot below (Fig. 6).

Contrary to other models, the pseudo-second-order equation hypothesizes that the adsorption capacity is proportional to the number of active sites occupied on the adsorbent. The linearized form of the pseudo-second-order model may be expressed as:

Table 1
Parameters of linearized Langmuir, Freundlich and Temkin isotherms for adsorption of Pb(II) onto PF-TWPs

T (K)	Langmuir isotherms			Freundlich isotherms			Temkin isotherms		
	b_L	Q_{max}	R^2	1/*n*	K_A	R^2	A_T	*B*	R^2
298	0.034	66.66	0.986	0.663	3.41	0.99	2.14	12.90	0.96
308	0.026	68.02	0.980	0.698	2.67	0.996	2.52	12.33	0.95
318	0.021	72.46	0.974	0.748	2.09	0.998	2.88	12.13	0.94

Table 2
Comparison of different adsorbent in terms of adsorption capacities of Pb(II)

Adsorbent	Q_{max} (mg g^{-1})	pH	Reference
Pine cone activated carbon	27.53	6.7	[41]
Ladle furnace steel dust	208.9	4.5	[42]
Peat	82.31	5	[43]
Banana peels biochar	247.1	6	[44]
Cauliflower leaves biochar	177.8	6	[44]
Date seed biochar	44.5	6	[45]
Hierarchical porous biochar	133.6	5	[46]
Nitro-oxidized carboxycellulose nanofibers	2,270	7	[47]
HNO_3-modified *P. americana* L	12.66	6	[48]
Phytolacca americana L	10.83	6	[48]
Xanthated *Lagenaria vulgaris* shell	33.21	5	[49]
Chitosan loaded MnO_2 nanoparticles	126.1	4	[50]
PF-TWPs	72.46	5.5	This study

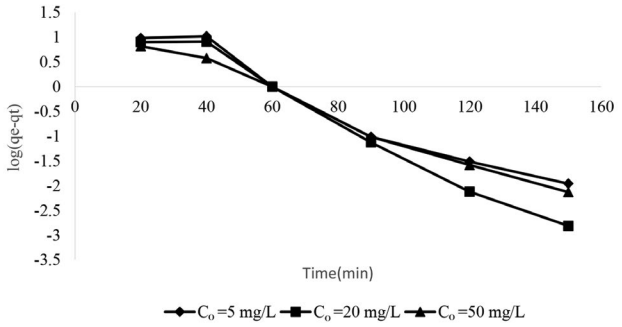

Fig. 6. Lagergren's plots for the adsorption of Pb(II) at varying Pb(II) concentrations.

$$\frac{t}{q_t} = \frac{1}{k_2 q_e^2} + \frac{1}{q_e} t \tag{8}$$

where k_2 is the rate constant of pseudo-second-order adsorption (g mg^{-1} min^{-1}) and can be estimated by the t/q_t vs. t plot (Fig. 7a).

The intraparticle diffusion model includes multiple steps and indicates that sharper (initial) portion is the external surface adsorption, the second portion is the gradual adsorption, and the third portion has to do with the final equilibrium. According to Weber and Morris [54] the intraparticle diffusion model is obtained by the following equation:

$$q_t = k_i t^{1/2} + C \tag{9}$$

where k_i is the intra-particle diffusion rate constant (mg g^{-1} min$^{-1/2}$), which can be calculated from the linear plots of q_t vs. $t^{1/2}$ (Fig. 7b).

The calculated parameters of adsorption kinetics equations are shown in Table 3. The experimental data of adsorption kinetic of the Pb(II) onto PF-TWPs showed that the pseudo-second-order kinetic model was well-fitted

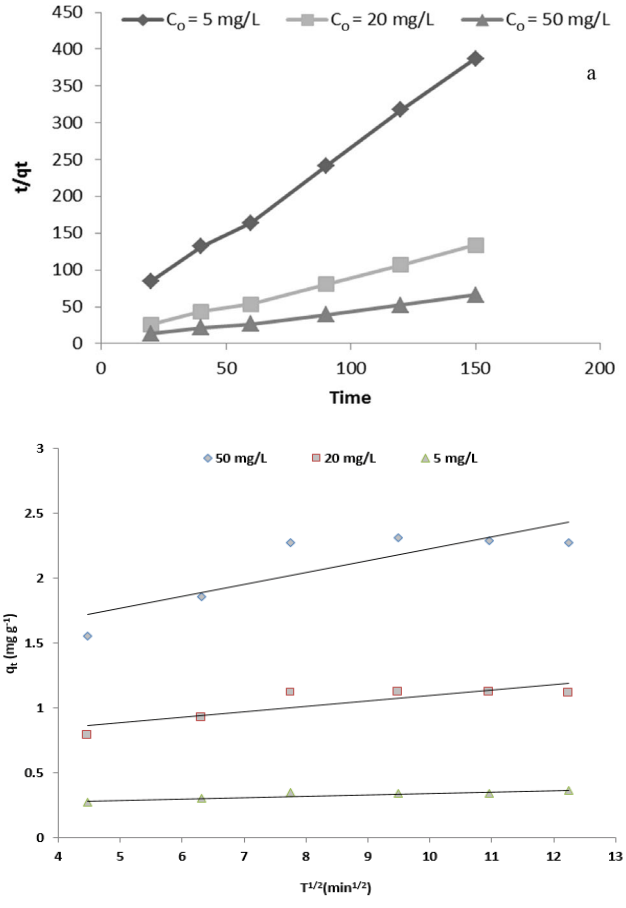

Fig. 7. (a) Pseudo-second-order and (b) intraparticle diffusion kinetics plots at varying Pb(II) concentration.

owing to the highest R^2 values (≥0.99). Furthermore, the pseudo-second-order kinetics model provided a relatively appropriate relationship between the theoretical and experimental q_e values. The increase in the rate constant,

Table 3
Kinetic parameters for the removal of Pb(II) by PF-TWPs

Initial concentration	Pseudo-first-order			Pseudo-second-order			Intraparticle diffusion
	k_1 (min^{-1})	q_e	R^2	k_2 (g mg^{-1} min^{-1})	q_e	R^2	k_i (mg g^{-1} min$^{-1/2}$)
5	0.058	0.024	0.95	0.012	2.347	0.997	0.010
20	0.072	0.015	0.97	0.087	0.828	0.996	0.041
50	0.055	0.041	0.98	0.183	0.405	0.994	0.091

k_2, (from 0.012 to 0.183 g mg^{-1} min^{-1}) was associated with increasing the initial concentrations of Pb(II) (from 5 to 50 mg L^{-1}). Regarding this, the adsorption capacity of equilibrium showed dependency on the initial concentration of Pb(II).

With respect to the results, the rate-limiting step is thought to occur during the chemisorption process. It was also shown that the intraparticle diffusion constant (k_i) for adsorption of Pb(II) at different concentrations onto PF-TWPs consists of two stages [55]. First, sharp linear curves are attributed to the diffusion of lead ions through the solution film to the external surface of pulp fibers, and second, the diffusion of Pb(II) onto macrospores, wider and smaller mesopores, and microspores adsorption site.

To describe and determine the adsorption mechanism, we can be applied of Boyd model in which that shown linearly as:

$$Bt = -\ln\frac{\pi^2}{6} - \ln\left(1 - F(t)\right) \tag{10}$$

where F is Pb(II) adsorbed onto PF-TWPs during different times that can be obtained as:

$$F = \frac{q_t}{q_e} \tag{11}$$

If we are drawing the plot of B_t vs. t, related parameters obtained by calculating the intercept and slope of a straight line of the plot. According to considering assumption in the Boyd model, the predominant mechanism (film diffusion or external mass transport) of adsorption will be obtained from being linear or nonlinear of the plot. As shown in Fig. 8, the adsorption following from the film – diffusion mechanism based on the being linear of the curve.

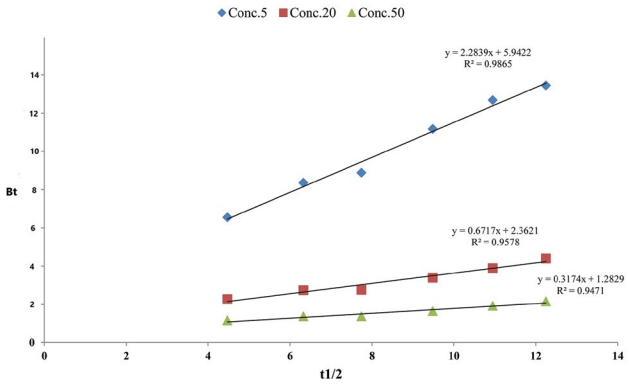

Fig. 8. The plot of Boyd model for the PF-TWPs.

3.7. Thermodynamic studies

Thermodynamic parameters, including enthalpy ($\Delta H°$), the Gibbs free energy change ($\Delta G°$), and entropy change ($\Delta S°$), were used to not only check if the process of Pb(II) adsorption onto PF-TWPs spontaneously occurs, but also identify the effect of temperature on this process. These parameters were estimated through the following equations [36]:

$$\text{Ln } k_0 = \frac{\Delta S°}{R} - \frac{\Delta H°}{RT} \tag{12}$$

$$\Delta G° = -RT \ln k_0 \tag{13}$$

where k_0 is the thermodynamic equilibrium constant corresponding to the temperatures of 298, 308 and 318 K, derived from plotting a straight line of ln (q_e/C_e) vs. q_e, and extrapolating q_e to zero, R is the universal gas constant (8.314 J mol^{-1} K^{-1}), and T is the absolute temperature (K).

The values of $\Delta H°$ and $\Delta S°$ were estimated from the slope and intercept of the linear plot of lnk_0 vs. 1/T). As demonstrated in Table 4, with calculating the negative values of $\Delta G°$ at all temperatures for PF-TWPs, the feasibility and spontaneity of the adsorption process in the natural conditions were approved. It was also indicated that the quantity of Gibbs free energy increased as the temperature increased. The raise in the randomness of the solid-solution interface could be explained by the observation of positive changes in standard entropy value ($\Delta S°$) during the course of Pb(II) adsorption onto PF-TWPs. Regarding the $\Delta H°$ positive value which was estimated in the current study, the endothermic nature of the process could be concluded, which was arisen

Table 4
Thermodynamic parameters of Pb(II) on PF-TWPs

T (K)	ΔG (kJ mol^{-1})	ΔH (kJ mol^{-1})	ΔS (kJ mol^{-1} K^{-1})
298	–5.577		
308	–6.476	19.89	0.085
318	–7.278		

from Pb(II) ions and PF-TWPs surface interactions. Besides, this process might be referred to as the deprotonation reaction and the process of diffusion.

It is worth saying that the results of the removal of heavy metals by paper waste can be promising and could be more friendly than other processes such as the application of ion exchange and electrocoagulation [56–58].

4. Conclusion

The findings of this study revealed that the modification process was performed in order to change the waste papers to new products. Based on PH analysis, the maximum Pb(II) removal (72.46 mg g^{-1}) from aqueous solutions was achieved at PH 5.5. This study showed that based on total selected temperature ranges and the initial concentration of Pb(II), the Freundlich isotherm and pseudo-second-order kinetic models, respectively, were fitted more appropriately with our experimental data. The negative (for $\Delta G°$) and positive values (for $\Delta H°$) obtained by thermodynamic analyses proved the spontaneity and endothermicity nature of Pb(II) adsorption process, respectively. Moreover, with regard to desorption studies, the adsorbent was found to be reusable. It can also be concluded that a 72% recovery of Pb(II) from PF-TWPs could be achieved by 1 M HCl. Following this recovery, the adsorption capacity of PF-TWPs for the removal of Pb(II) from aqueous solutions decreased by 12% on average (The data related to Recovery Pb(II) from PF-TWPs after adsorption showed supplementary materials). To sum up, waste papers as available and plentiful materials, after undergoing some modifications which were conducted in our study, could be used as an effective and low-cost adsorbent for the removal of lead from aqueous solutions. This newly expanded adsorbent was successfully employed in the treatment of Pb(II) – containing effluents arisen from industries, with the capability of removing other heavy metals and pollutants.

Acknowledgments

This study is related to the project by No. 1396/89342 from the Student Research Committee, Shahid Beheshti University of Medical Sciences, Tehran, Iran. We appreciate the "Student Research Committee" and "Research & Technology Chancellor" in Shahid Beheshti University of Medical Sciences for their financial support of this study. The authors would also like to express their gratitude to Farid Solaymani-Mohammadi for his great contribution in writing and grammatical revision of the manuscript.

References

[1] Y. Hang, Y. Si, Q. Zhou, H.B. Yin, A. Wang, A. Cao, Morphology-controlled synthesis of calcium titanate particles and adsorption kinetics, isotherms, and thermodynamics of Cd(II), Pb(II), and Cu(II) cations, J. Hazard. Mater., 380 (2019) 120789.
[2] A.H. Mahvi, F. Gholami, S. Nazmara, Cadmium biosorption from wastewater by *Ulmus* leaves and their ash, Eur. J. Sci. Res., 23 (2008) 197–203.
[3] H. Benhima, M. Chiban, F. Sinan, P. Seta, M. Persin, Removal of lead and cadmium ions from aqueous solution by adsorption onto micro-particles of dry plants, Colloids Surf., B, 61 (2008) 10–16.
[4] A. Maleki, A.H. Mahvi, M.A. Zazouli, H. Izanloo, A.H. Barati, Aqueous cadmium removal by adsorption on barley hull and barley hull ash, Asian J. Chem., 23 (2011) 1373–1376.
[5] E. Bazrafshan, L. Mohammadi, A. Ansari-Moghaddam, A.H. Mahvi, Heavy metals removal from aqueous environments by electrocoagulation process–a systematic review, J. Environ. Health Sci. Eng., 13 (2015), https://doi.org/10.1186/s40201-015-0233-8.
[6] W.S. Wan Ngah, M.A.K.M. Hanafiah, Removal of heavy metal ions from wastewater by chemically modified plant wastes as adsorbents: a review, Bioresour. Technol., 99 (2008) 3935–3948.
[7] A.P. Lim, A.Z. Aris, Continuous fixed-bed column study and adsorption modeling: removal of cadmium(II) and lead(II) ions in aqueous solution by dead calcareous skeletons, Biochem. Eng. J., 87 (2014) 50–61.
[8] Y. Bulut, Z. Tez, Removal of heavy metals from aqueous solution by sawdust adsorption, J. Environ. Sci., 19 (2007) 160–166.
[9] M.S. Rahman, M.R. Islam, Effects of pH on isotherms modeling for Cu(II) ions adsorption using maple wood sawdust, Chem. Eng. J., 149 (2009) 273–280.
[10] H.J. Mansoorian, A.H. Mahvi, A.J. Jafari, Removal of lead and zinc from battery industry wastewater using electrocoagulation process: influence of direct and alternating current by using iron and stainless steel rod electrodes, Sep. Purif. Technol., 135 (2014) 165–175.
[11] M.K. Mondal, Removal of Pb(II) from aqueous solution by adsorption using activated tea waste, Korean J. Chem. Eng., 27 (2010) 144–151.
[12] L. Zhang, X. Liu, W. Wang, Y. Li, P. Sun, S. Shang, Q. Jiang, Characteristics and mechanism of lead adsorption from aqueous solutions by oil crops straw-derived biochar, Trans. CSAE, 34 (2018) 218–226.
[13] M. Sharma, J. Singh, S. Hazra, S. Basu, Adsorption of heavy metal ions by mesoporous ZnO and TiO_2@ZnO monoliths: adsorption and kinetic studies, Microchem. J., 145 (2019) 105–112.
[14] L.Z. Zou, P.H. Shao, K. Zhang, L.M. Yang, D. You, H. Shi, S.G. Pavlostathis, W.Q. Lai, D.H. Liang, X.B. Luo, Tannic acid-based adsorbent with superior selectivity for lead(II) capture: adsorption site and selective mechanism, Chem. Eng. J., 364 (2019) 160–166.
[15] M. Imamoglu, O. Tekir, Removal of copper(II) and lead(II) ions from aqueous solutions by adsorption on activated carbon from a new precursor hazelnut husks, Desalination, 228 (2008) 108–113.
[16] L. Largitte, S. Gervelas, T. Tant, P.C. Dumesnil, A. Hightower, R. Yasami, Y. Bercion, P. Lodewyckx, Removal of lead from aqueous solutions by adsorption with surface precipitation, Adsorption, 20 (2014) 689–700.
[17] S.-G. Wang, W.-X. Gong, X.-W. Liu, Y.-W. Yao, B.-Y. Gao, Q.-Y. Yue, Removal of lead(II) from aqueous solution by adsorption onto manganese oxide-coated carbon nanotubes, Sep. Purif. Technol., 58 (2007) 17–23.
[18] J.J. Moreno-Barbosa, C. López-Velandia, A. del Pilar Maldonado, L. Giraldo, J.C. Moreno-Piraján, Removal of lead(II) and zinc(II) ions from aqueous solutions by adsorption onto activated carbon synthesized from watermelon shell and walnut shell, Adsorption, 19 (2013) 675–685.
[19] A. Demirbas, Heavy metal adsorption onto agro-based waste materials: a review, J. Hazard. Mater., 157 (2008) 220–229.
[20] S.E. Bailey, T.J. Olin, R.M. Bricka, D.D. Adrian, A review of potentially low-cost sorbents for heavy metals, Water Res., 33 (1999) 2469–2479.
[21] M. Jalali, F. Aboulghazi, Sunflower stalk, an agricultural waste, as an adsorbent for the removal of lead and cadmium from aqueous solutions, J. Mater. Cycles Waste Manage., 15 (2013) 548–555.
[22] H.B. Bradl, Adsorption of heavy metal ions on soils and soils constituents, J. Colloid Interface Sci., 277 (2004) 1–18.
[23] F.L. Fu, Q. Wang, Removal of heavy metal ions from wastewaters: a review, J. Environ. Manage., 92 (2011) 407–418.

[24] T.A. Kurniawan, G.Y.S. Chan, W.-h. Lo, S. Babel, Comparisons of low-cost adsorbents for treating wastewaters laden with heavy metals, Sci. Total Environ., 366 (2006) 409–426.
[25] M. Kobya, E. Demirbas, E. Senturk, M. Ince, Adsorption of heavy metal ions from aqueous solutions by activated carbon prepared from apricot stone, Bioresour. Technol., 96 (2005) 1518–1521.
[26] F.Y. Wang, H. Wang, J.W. Ma, Adsorption of cadmium(II) ions from aqueous solution by a new low-cost adsorbent—bamboo charcoal, J. Hazard. Mater., 177 (2010) 300–306.
[27] M.A. Ferro-García, J. Rivera-Utrilla, J. Rodríguez-Gordillo, I. Bautista-Toledo, Adsorption of zinc, cadmium, and copper on activated carbons obtained from agricultural by-products, Carbon, 26 (1988) 363–373.
[28] A. Bhatnagar, A.K. Minocha, M. Sillanpää, Adsorptive removal of cobalt from aqueous solution by utilizing lemon peel as biosorbent, Biochem. Eng. J., 48 (2010) 181–186.
[29] G. Sun, W.X. Shi, Sunflower stalks as adsorbents for the removal of metal ions from wastewater, Ind. Eng. Chem. Res., 37 (1998) 1324–1328.
[30] A.H. Mahvi, Application of agricultural fibers in pollution removal from aqueous solution, Int. J. Environ. Sci. Technol., 5 (2008) 275–285.
[31] M.H. Ehrampoush, M. Miria, M.H. Salmani, A.H. Mahvi, Cadmium removal from aqueous solution by green synthesis iron oxide nanoparticles with tangerine peel extract, J. Environ. Health Sci. Eng., 84 (2015) 13.
[32] B. Kakavandi, R.R. Kalantary, M. Farzadkia, A.H. Mahvi, A. Esrafili, A. Azari, A.R. Yari, A.B. Javid, Enhanced chromium(VI) removal using activated carbon modified by zero valent iron and silver bimetallic nanoparticles, J. Environ. Health Sci. Eng., 12 (2014) 115.
[33] M.H. Dehghani, D. Sanaei, I. Ali, A. Bhatnagar, Removal of chromium(VI) from aqueous solution using treated waste newspaper as a low-cost adsorbent: kinetic modeling and isotherm studies, J. Mol. Liq., 215 (2016) 671–679.
[34] N.A. Nikonenko, D.K. Buslov, N.I. Sushko, R.G. Zhbankov, Investigation of stretching vibrations of glycosidic linkages in disaccharides and polysaccharides with use of IR spectra deconvolution, Biopolymers, 57 (2000) 257–262.
[35] D.M. Suflet, G.C. Chitanu, V.I. Popa, Phosphorylation of polysaccharides: new results on synthesis and characterisation of phosphorylated cellulose, React. Funct. Polym., 66 (2006) 1240–1249.
[36] M.H. Dehghani, M. Sarmadi, M.R. Alipour, D. Sanaei, H. Abdolmaleki, S. Agarwal, V.K. Gupta, Investigating the equilibrium and adsorption kinetics for the removal of Ni(II) ions from aqueous solutions using adsorbents prepared from the modified waste newspapers: a low-cost and available adsorbent, Microchem. J., 146 (2019) 1043–1053.
[37] L.P. Lingamdinne, J.R. Koduru, Y.-Y. Chang, R.R. Karri, Process optimization and adsorption modeling of Pb(II) on nickel ferrite-reduced graphene oxide nano-composite, J. Mol. Liq., 250 (2018) 202–211.
[38] R.I. Masel, Principles of Adsorption and Reaction on Solid Surfaces, John Wiley & Sons, 1996.
[39] C. Ng, J.N. Losso, W.E. Marshall, R.M. Rao, Freundlich adsorption isotherms of agricultural by-product-based powdered activated carbons in a geosmin–water system, Bioresour. Technol., 85 (2002) 131–135.
[40] M. Temkin, Kinetics of ammonia synthesis on promoted iron catalysts, Acta Physiochim. URSS, 12 (1940) 327–356.
[41] M. Momčilović, M. Purenović, A. Bojić, A. Zarubica, M. Ranđelović, Removal of lead(II) ions from aqueous solutions by adsorption onto pine cone activated carbon, Desalination, 276 (2011) 53–59.
[42] Z.B. Bouabidi, M.H. El-Naas, D. Cortes, G. McKay, Steel-making dust as a potential adsorbent for the removal of lead(II) from an aqueous solution, Chem. Eng. J., 334 (2018) 837–844.
[43] P. Bartczak, M. Norman, Ł. Klapiszewski, N. Karwańska, M. Kawalec, M. Baczyńska, M. Wysokowski, J. Zdarta, F. Ciesielczyk, T. Jesionowski, Removal of nickel(II) and lead(II) ions from aqueous solution using peat as a low-cost adsorbent: a kinetic and equilibrium study, Arabian J. Chem., 11 (2018) 1209–1222.
[44] Z. Ahmad, B. Gao, A. Mosa, H.W. Yu, X.Q. Yin, A. Bashir, H. Ghoveisi, S.S. Wang, Removal of Cu(II), Cd(II) and Pb(II) ions from aqueous solutions by biochars derived from potassium-rich biomass, J. Cleaner Prod., 180 (2018) 437–449.
[45] Z. Mahdi, Q.J. Yu, A. El Hanandeh, Competitive adsorption of heavy metal ions (Pb^{2+}, Cu^{2+}, and Ni^{2+}) onto date seed biochar: batch and fixed bed experiments, Sep. Sci. Technol., 54 (2019) 888–901.
[46] W.Q. Yin, D. Dai, J.H. Hou, S.S. Wang, X.G. Wu, X.Z. Wang, Hierarchical porous biochar-based functional materials derived from biowaste for Pb(II) removal, Appl. Surf. Sci., 465 (2019) 297–302.
[47] P.R. Sharma, A. Chattopadhyay, C.B. Zhan, S.K. Sharma, L.H. Geng, B.S. Hsiao, Lead removal from water using carboxycellulose nanofibers prepared by nitro-oxidation method, Cellulose, 25 (2018) 1961–1973.
[48] G.Y. Wang, S.R. Zhang, P. Yao, Y. Chen, X.X. Xu, T. Li, G.S. Gong, Removal of Pb(II) from aqueous solutions by *Phytolacca americana* L. biomass as a low cost biosorbent, Arabian J. Chem., 11 (2018) 99–110.
[49] M. Kostić, M. Radović, J. Mitrović, M. Antonijević, D. Bojić, M. Petrović, A. Bojić, Using xanthated *Lagenaria vulgaris* shell biosorbent for removal of Pb(II) ions from wastewater, J. Iran Chem. Soc., 11 (2014) 565–578.
[50] V.-P. Dinh, N.-C. Le, L.A. Tuyen, N.Q. Hung, V.-D. Nguyen, N.-T. Nguyen, Insight into adsorption mechanism of lead(II) from aqueous solution by chitosan loaded MnO_2 nanoparticles, Mater. Chem. Phys., 207 (2018) 294–302.
[51] I. Langmuir, The adsorption of gases on plane surfaces of glass, mica and platinum, J. Am. Chem. Soc., 40 (1918) 1361–1403.
[52] P. Patnukao, A. Kongsuwan, P. Pavasant, Batch studies of adsorption of copper and lead on activated carbon from *Eucalyptus camaldulensis* dehn. bark, J. Environ. Sci.–China, 20 (2008) 1028–1034.
[53] J. Wu, H. Zhang, P.-J. He, Q. Yao, L.-M. Shao, Cr(VI) removal from aqueous solution by dried activated sludge biomass, J. Hazard. Mater., 176 (2010) 697–703.
[54] W.J. Weber, J.C. Morris, Kinetics of adsorption on carbon from solution, J. Sanit. Eng. Div., Proc. Am. Soc. Civ. Eng., 89 (1963) 31–60.
[55] P. Kampalanonwat, P. Supaphol, Preparation and adsorption behavior of aminated electrospun polyacrylonitrile nanofiber mats for heavy metal ion removal, ACS Appl. Mater. Interfaces, 2 (2010) 3619–3627.
[56] L. Rafati, A.H. Mahvi, A.R. Asgari, S.S. Hosseini, Removal of chromium(VI) from aqueous solutions using Lewatit FO36 nano ion exchange resin, Int. J. Environ. Sci. Technol., 7 (2010) 147–156.
[57] M.R. Boldaji, A.H. Mahvi, S. Dobaradaran, S.S. Hosseini, Evaluating the effectiveness of a hybrid sorbent resin in removing fluoride from water, Int. J. Environ. Sci. Technol., 6 (2009) 629–632.
[58] E. Bazrafshan, A.H. Mahvi, M.A. Zazouli, Removal of zinc and copper from aqueous solutions by electrocoagulation technology using iron electrodes, Asian J. Chem., 23 (2011) 5506.

Supplementary information

S1. Characterization of phosphate-functionalized treated waste papers

S1.1. Waste paper pulps and phosphate-functionalized treated waste papers surface area properties

Brunauer–Emmett–Teller (BET) method was used to measure the surface area of waste papers (WPs) and phosphate-functionalized treated waste papers (PF-TWPs) via BET, surface area analysis (TriStar 3000, Micromeritics, surface area and pore size analyzer, U.S. Sales). Given the scanning electron microscopy analysis of WPs and PF-TWPs, fibers whose space is filled with agglomerated fine particles have been shown to constitute the microstructures of newspapers. There was a S_{BET} value of WPs ranging from 885 to 1,020 $m^2\ g^{-1}$, with a 1,214–1,652 $m^2\ g^{-1}$ specific surface area for PF-TWPs determined via chemical analysis which verified phosphorous impregnation upon chemical treatment. The values of pore volume for WPs were determined to 0.98 mL g^{-1}, with a value of 1.01 mL g^{-1} for PF-TWPs.

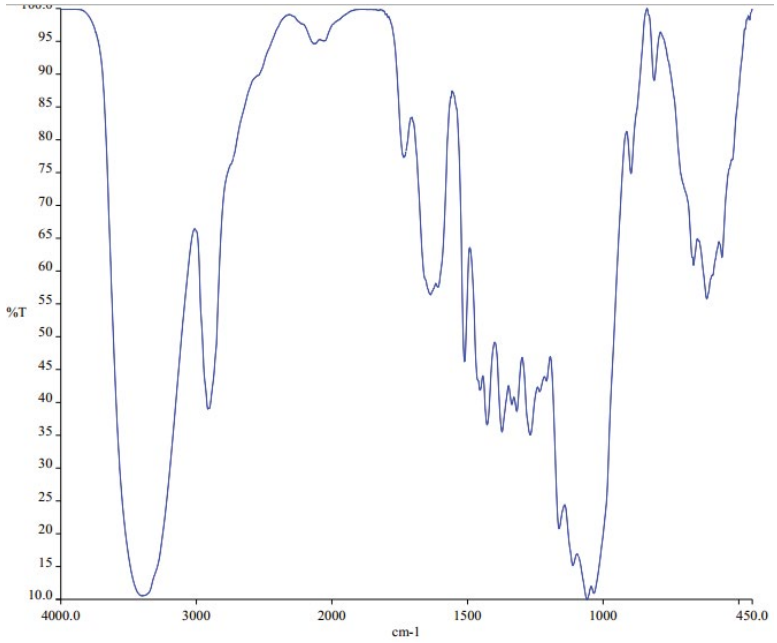

Fig. S1. Fourier-transform infrared spectrum of waste papers.

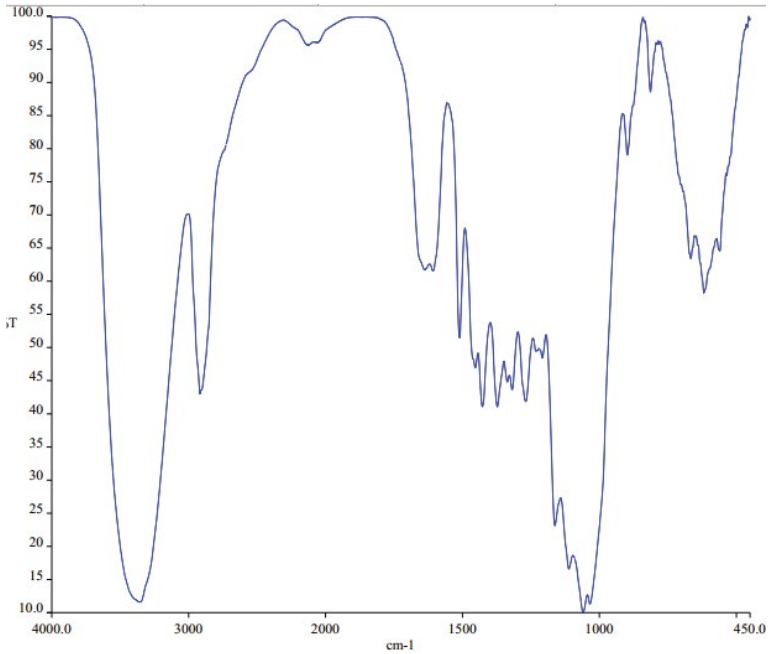

Fig. S2. Fourier-transform infrared spectrum of treated waste papers with phosphate-functionalized.

Table S1
Mean elemental concentration in treated waste papers obtained by energy dispersive X-ray fluorescence

Element	Sample	Limit of detection (LOD)
Cd	<LOD	0.003
Hg	<LOD	0.005
Ba	<LOD	0.007
Cr	<LOD	0.109
Sb	<LOD	0.003
Se	<LOD	0.003
Ag	<LOD	0.003
Mo	<LOD	0.032
Nb	<LOD	0.12
Zr	<LOD	0.025
Bi	<LOD	0.003
Sn	<LOD	0.003
Br	<LOD	0.003
Pd	<LOD	0.003
Au	<LOD	0.009
Pt	<LOD	0.01
Zn	0.035	0.005
Cu	<LOD	0.009
Ni	<LOD	0.014
Co	<LOD	0.015
Fe	<LOD	0.033
Mn	<LOD	0.061
In	<LOD	0.003
V	<LOD	0.218
Ti	<LOD	0.435
Pb	<LOD	0.003

S1.2. Regeneration of PF-TWPs

The recovery of lead(II) from the adsorbent was performed using 0.01, 0.1, and 1.0 M HCl solution. The adsorbent dose of 1 g was loaded with 250 ml of 20 mg L^{-1} of lead solution. The Pb(II) was adsorbed by PF-TWPs and desorption studies attempted to recover Pb(II) from metal ion loaded adsorbent for the above-mentioned concentration. The results show that 72% of the adsorbed Pb(II) was desorbed from PF-TWPs using 0.1 M HCl. During desorption studies, the PF-TWPs surface was completely covered by H^+ ions. It is evident from Fig. S4, that the regeneration of PF-TWPs resulted in the release of Pb(II) ions from adsorbent's surface to the solution and regenerated PF-TWPs can be reused for Pb(II) removal from aqueous solution.

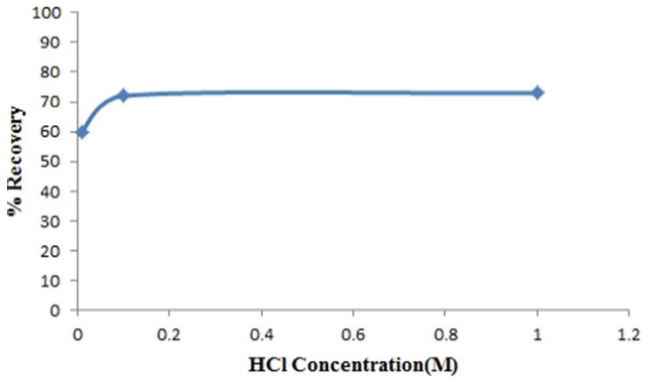

Fig. S4. The regeneration study of PF-TWPs

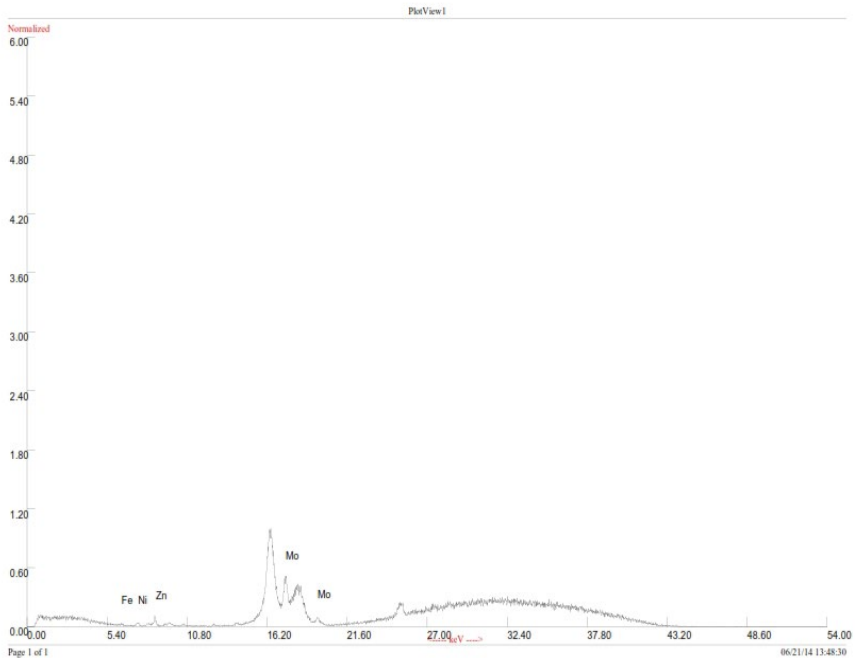

Fig. S3. Mean elemental concentration in PF-TWPs by energy dispersive X-ray fluorescence.